JACS
JOURNAL OF THE AMERICAN CHEMICAL SOCIETY
Article
pubs.acs.org/JACS

Crystal Structure Control of Zinc-Blende CdSe/CdS Core/Shell Nanocrystals: Synthesis and Structure-Dependent Optical Properties

Wennuan Nan, Yuan Niu, Haiyan Qin,* Fan Cui, Yu Yang, Runchen Lai, Wanzhen Lin, and Xiaogang Peng*

Department of Chemistry, Zhejiang University, Hangzhou, 310027, P. R. China

Supporting Information

ABSTRACT: Nearly monodisperse zinc-blende CdSe/CdS core/shell nanocrystals were synthesized by epitaxial growth of 1−6 monolayers of CdS shell onto presynthesized zinc-blende CdSe core nanocrystals in one pot. To retain the zinc-blende structure, the reaction temperature was lowered to the 100−140 °C range by using cadmium diethyldithiocarbamate as a single-source precursor and primary amine as activation reagents for the precursor. Although the wurtzite counterparts grown under the same conditions showed optical properties similar to those reported in the literature, zinc-blende CdSe/CdS core/shell nanocrystals demonstrated surprisingly different optical properties, with ensemble single-exponential photoluminescence decay, significant decrease of photoluminescence peak width by the shell growth, and comparatively high photoluminescence quantum yields. The lifetime for the single-exponential ensemble photoluminescence decay of zinc-blende CdSe/CdS core/shell nanocrystals with 3−4 monolayers of CdS shell was reproducibly found to be approximately 16.5 ± 1.0 ns.

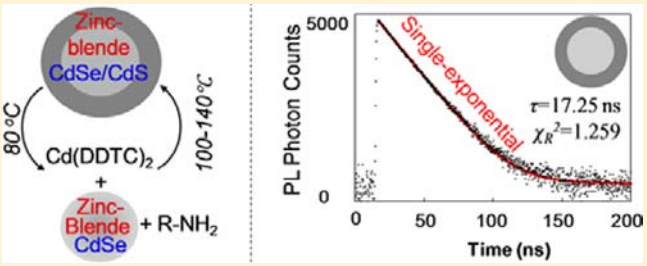

INTRODUCTION

Synthesis of high-quality colloidal semiconductor nanocrystals in their quantum confinement size regime (quantum dots) has become a major research subject in the field of materials chemistry because of their unique size-dependent properties, especially emissive properties.[1,2] High photoluminescence (PL) quantum yield (QY) of II−VI quantum dots (>50%) has been reported repeatedly in the literature.[3,4] Bright quantum dots could presumably withstand application conditions[5−9] after they are made into core/shell structures. Emission of colloidal quantum dots is due to radiative recombination of the electron−hole pair called exciton. In a semiconductor nanocrystal, the wave function of the exciton is delocalized and can thus be affected by possible structure defects. As a result, core/shell quantum dots very likely need to be made with precise control by epitaxial growth, which unfortunately is still mostly empirical.[10−14] For instance, although mostly studied CdSe nanocrystals could be made in both wurtzite (hexagonal)[4] and zinc-blende (cubic)[15] crystal structures with high quality, epitaxial growth of other semiconductor materials onto zinc-blende CdSe core nanocrystals has only achieved limited success.[16−18] For instance, it has been noticed that, starting from zinc-blende CdSe core nanocrystals, the resulting core/shell nanocrystals often could not retain the original crystal structure.[17,19,20] This and other types of poor control of crystal structure during epitaxial growth might yield core/shell nanocrystals without desired optical properties, especially emissive properties. For example, the Krauss research group[21] reported that blinking behavior of single-dot PL of CdSe-based core/shell nanocrystals was strongly affected by the control of shell composition. For the mostly studied CdSe/CdS core/shell nanocrystal system, there are no comparative studies on their crystal-structure-dependent optical properties likely due to the lack of zinc-blende CdSe/CdS core/shell nanocrystals with high optical quality.

Bulk CdSe and CdS can both appear in either the zinc-blende (cubic) or wurtzite (hexagonal) crystal structure, four of which are all tetrahedron coordination in terms of chemical bonding. For both types of crystal structures, the lattice constants of bulk CdSe and CdS differ from each other by about 4%. The bulk CdSe bandgap (~1.72 eV) is significantly smaller than that of bulk CdS (~2.5 eV). The band offset between bulk CdSe and CdS is type-I, meaning that the bottom of the conduction band of bulk CdS is higher than that of bulk CdSe, while the top of the valence band of CdS is lower than that of bulk CdSe. As mentioned above, the CdSe/CdS core/shell nanocrystal system is the mostly studied core/shell dot system for its outstanding optical properties, especially after the discovery of suppression of single-dot PL blinking in wurtzite CdSe/CdS core/shell dots with very thick CdS shells.[14,22]

In classic crystallization literature, it is well-known that, for CdSe and CdS, zinc-blende structure is more stable at low temperatures. This reminded us that the reaction temperatures used in the attempts at growing zinc-blende CdSe/CdS core/shell nanocrystals, usually at 200 °C or above,[16−20] might be too high. Two issues must be considered if one wants to reduce epitaxial growth temperature. First, the ligands must be labile

Received: July 8, 2012
Published: November 6, 2012

   dx.doi.org/10.1021/ja306651x | J. Am. Chem. Soc. 2012, 134, 19685−19693

yet provide sufficient dynamic surface passivation at reduced temperature to ensure both colloidal stability and appreciable growth.[23] Second, the precursors must be reactive for epitaxial growth at reduced temperatures yet not so reactive to cause self-nucleation.

In this report, we demonstrate that cadmium diethyldithiocarbamate ($Cd(DDTC)_2$), similar to zinc diethyldithiocarbamate ($Zn(DDTC)_2$) used for shell growth for CdS/ZnS core/shell nanocrystals,[24,25] could afford growth of high-quality CdSe/CdS core/shell nanocrystals with zinc-blende crystal structure at least up to six monolayers of CdS. Furthermore, a similar scheme could also be used for epitaxial growth of their wurtzite counterparts. The key is to successfully reduce the reaction temperature to the range between 100 and 140 °C by applying primary amine as activation reagents and dynamic ligands. Although recent reports suggested that primary fatty amines presented in the growth solution might have played a decisive role in converting zinc-blende CdSe core nanocrystals to wurtzite ones during the growth of the CdS shell,[17] the results shown below will demonstrate that the primary amines in our system did not drive such a conversion. Successful synthesis of high-quality CdSe/CdS core/shell nanocrystals with both zinc-blende and wurtzite structures enabled us to study the crystal structure dependence of their optical properties. The results to be described below shall reveal that optical properties of the zinc-blende CdSe/CdS core/shell nanocrystals were substantially different from those of their wurtzite counterparts.

RESULTS AND DISCUSSION

Choice of Reaction System. Although the main focus of this work was on zinc-blende CdSe/CdS core/shell nanocrystals, growth of the wurtzite counterparts under the same conditions was carried out as a comparative system. High-quality CdSe core nanocrystals with either zinc-blende[15] or wurtzite[4] structure were synthesized following literature methods. Single-source precursors with coordination structure similar to that of cadmium diethyldithiocarbamate ($Cd(DDTC)_2$) but different hydrocarbon parts were examined. Results showed that $Cd(DDTC)_2$ gave us desired reactivity for epitaxial growth at reduced temperatures. Although the commonly used noncoordinating solvent, octadecene (ODE), worked as the reaction solvent, octane was found to give significantly better postsynthesis handling. Fatty amines were used as both activation reagents for the single-source precursor[25] and surface ligands for the nanocrystals. In the literature, amine-activated decomposition of $Zn(DDTC)_2$ under elevated temperature was reported.[26] Although it is unclear whether a similar decomposition pathway exists for $Cd(DDTC)_2$, the experimental results revealed that fatty amines greatly accelerated the CdS shell growth (see detail below).

The one-pot approach reported for the CdS/ZnS core/shell nanocrystal system[25] worked well in this work. However, the related purification procedure, extraction using the hexane/methanol biphase system, did not work for zinc-blende CdSe core nanocrystals at all. Additional precipitation following the extraction procedure using acetone did not change the situation. Finally, it was determined that addition of amine and tributylphosphine into the extraction solution was essential for effective removal of the unreacted precursors for formation of zinc-blende CdSe core nanocrystals, i.e., cadmium fatty acid salts and Se powder. Fourier transform infrared (FT-IR) measurements showed that fatty amines could form a methanol-soluble complex with cadmium fatty acid salts. Tributylphosphine functioned as the scavenger for the unreacted elemental Se.[27] A detailed purification procedure for the zinc-blende CdSe core nanocrystals is provided in the Experimental Section. The dramatic effects of purification will be discussed later.

After establishing a purification scheme for zinc-blende CdSe core nanocrystals, the reaction conditions were mostly optimized around reaction temperatures during the shell growth to achieve a balance between control of the crystal structure and appreciable epitaxial growth of the shell. Results revealed that it was difficult to maintain a zinc-blende structure under the traditional reaction temperature which was typically above 200 °C (see details below). During the revision of this manuscript, one referee reminded us of a report on growth of CdSe/CdS core/shell nanocrystals using $Cd(DDTC)_2$ as the single precursor.[18] However, the final reaction temperature in that report was set as 200 °C, which was found to be too high to maintain a zinc-blende structure in our experiments.

By varying the solution composition, $Cd(DDTC)_2$ could decompose well, while the reaction temperature was above 90 °C. To achieve control of epitaxial growth, we adopted a thermal-cycling technique coupled with single precursor (TC-SP).[25] That was to have a low temperature for addition of the precursor solution (80 °C) for the surface adsorption and a high temperature (in the range of 100−140 °C) for surface reaction/crystallization (Figure 1, left panel).

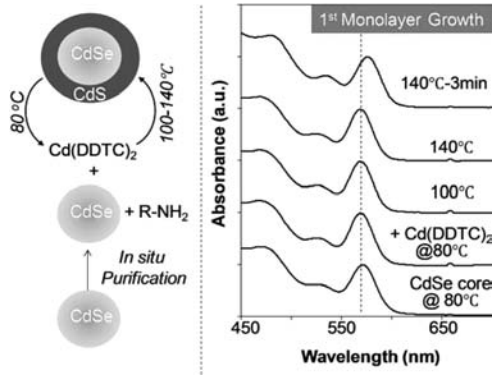

Figure 1. Left panel: schematic illustration of synthetic process. Right panel: temporal evolution of UV−vis spectra of quantum dots during the growth of the first monolayer of CdS onto CdSe core nanocrystals.

Interestingly, growth of the first monolayer of CdS needed a higher reaction temperature. For the typical reaction (see Experimental Section), the first monolayer needed to reach 140 °C for appreciable growth (Figure 1, right panel), and the consecutive monolayers grew well at about 120 °C. This could be caused by the partial retaining of the original carboxylate ligands on the core nanocrystals prior to the growth of the first monolayer of the CdS shell, and further experiments are in process to understand this growth temperature difference. It should be pointed out that the growth temperature of the CdS shell could be readily reduced to about 100 °C by further increasing the concentration of the primary amines in the reaction solution, indicating that a primary amine was indeed acting as the activation reagent for $Cd(DDTC)_2$.

The amount of precursors needed for each growth cycle for zinc-blende core/shell nanocrystals was initially calculated using

dx.doi.org/10.1021/ja306651x | J. Am. Chem. Soc. 2012, 134, 19685−19693

the extinction coefficients of wurtzite CdSe nanocrystals reported in the literature.[28] However, experimental results revealed that these extinction coefficients seemed to be underestimated. Besides, the intrinsic difference between zinc-blende and wurtzite crystal structure might further enlarge the inaccuracy.[29] While experiments are in process to determine extinction coefficients of zinc-blende CdSe nanocrystals, the thickness control in this work was accomplished by correlating UV−vis spectra with transmission electron microscopy (TEM) measurements.

Thickness-Dependent Optical Properties of Zinc-Blende CdSe/CdS Core/Shell Nanocrystals. Upon growth of the CdS shell onto CdSe nanocrystals, a continuous red shift of the first exciton absorption peak and band-edge PL peak was observed (Figure 2, left panel). The substantial red shift occurred for each monolayer of growth mostly as a consequence of exciton delocalization into the CdS shell region.[11] In the literature, such significant red shifts have been regarded as a signature of successful epitaxial growth of the shell, instead of serious alloying between the core and shell.[11]

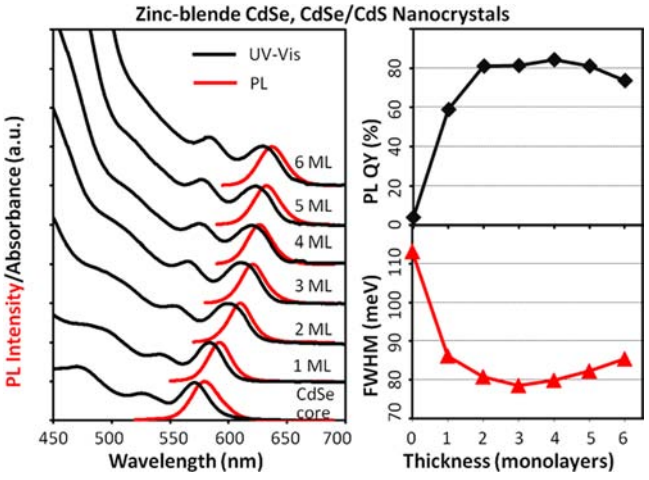

Figure 2. UV−vis and PL spectra (left panel), PL QY (top right), and fwhm (bottom right) of the PL peaks for the CdSe core (diameter = 3.5 nm) and CdSe/CdS core/shell nanocrystals with a given number of monolayers (ML) of the CdS shell.

The absolute PL quantum yield (QY) of nanocrystals was measured using an integrating sphere system (see details in the Experimental Section). Purified zinc-blende CdSe core nanocrystals had a very low PL QY, typically with a single-digit percentage. Since the PL QY of the core samples was measured using the nanocrystals right after the core purification process, the significant drop of the PL QY upon purification could be due to partial loss of the original carboxylate surface ligands on the core nanocrystals.

The first monolayer of the CdS shell substantially increased the PL QY of nanocrystals for the typical reaction shown in Figure 2. There was a continuous increase of PL QY as the thickness of the shell increased up to 4−5 monolayers (Figure 2, top right panel). This trend is similar to that observed for wurtzite CdSe/CdS core/shell nanocrystals reported in the literature.[13] It should be mentioned that, although the PL QY upon growth of the shell for a given reaction was found to vary with reaction conditions, values of zinc-blende CdSe/CdS core/shell nanocrystals were found reproducibly to be higher than those of wurtzite counterparts with the same PL peak position synthesized under the same conditions (see Figure S1, Supporting Information, and more detail below).

It was reported that metal dithiocarbamate decomposed into metal sulfide and H_2S,[26] and H_2S and the related species could subsequently be adsorbed onto the nanocrystals.[30] Such a surface might impact the optical properties of the nanocrystals. To test this, cadmium oleate was added into the reaction solution after the completion of each growth cycle. Results revealed that the PL QY usually increased noticeably for the first monolayer, and the effects of addition of cadmium oleate became less significant when the shell thickness reached about three monolayers. Furthermore, the addition of extra cadmium oleate in the early stage did not obviously affect the optical properties of the core/shell dots in the late stage. This indicates that the impact of surface states for zinc-blende CdSe/CdS core/shell nanocrystals was greatly reduced as the shell thickness was more than three monolayers.

The full width at half-maximum (fwhm) of PL peaks of the zinc-blende CdSe/CdS core/shell nanocrystals with thickness up to 6 monolayers of CdS was usually quite narrow. This implies that the size distribution of the final core/shell nanocrystals was nearly monodisperse. Interestingly, upon the growth of the shell, the fwhm of the PL peak decreased in the beginning, from >110 to <80 meV, and gradually increased when the thickness reached about 4−5 monolayers of CdS (Figure 2, bottom right). Furthermore, within 6 monolayers of CdS, the fwhm of the PL peak was always narrower than that of the original CdSe core nanocrystals, although transmission electron microscopy (TEM) studies revealed no noticeable change of their size distribution upon the shell growth (see below). A comparative study revealed that PL peak width narrowing upon growth of the CdS shell onto wurtzite CdSe core nanocrystals was not obvious (Figure S1, Supporting Information).

Bright zinc-blende CdSe/CdS core/shell nanocrystals (Figure 3, left) could be synthesized to cover the optical

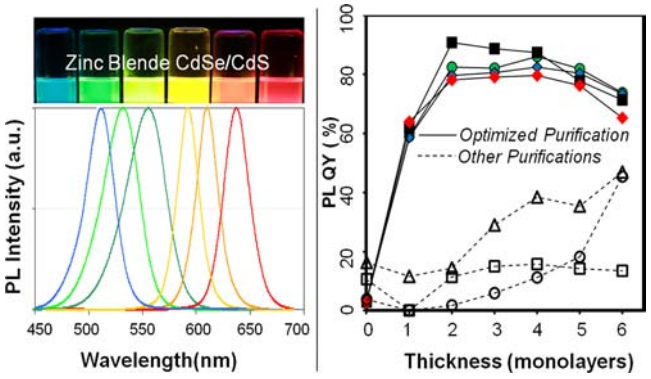

Figure 3. Left panel: Luminescence pictures under UV excitation (top) and PL spectra of zinc-blende CdSe/CdS core/shell nanocrystals with different emission wavelengths. Right panel: PL QY versus shell thickness for zinc-blende core and core/shell nanocrystals synthesized under different conditions. The experiments related to filled symbols in the plot were repeating synthetic runs using the optimized core purification procedure developed by this work (see text), and those associated with open symbols in the plot were carried out using other purification procedures (open squares, three times the hexane−methanol extraction; open triangles, acetone precipitation after three times of hexane−methanol extraction; and open circles, three times hexane−methanol extraction with the addition of fatty amines but without tributylphosphine).

dx.doi.org/10.1021/ja306651x | J. Am. Chem. Soc. 2012, 134, 19685−19693

window between lake blue to deep red (approximately from 500 to 650 nm). It should be pointed out that, because of the relatively poor control of size distribution of the small zinc-blende CdSe core nanocrystals (with their first exciton absorption peak below ~500 nm), the resulting core/shell nanocrystals with their emission color being blue and green usually possessed a relatively broad and sometimes asymmetric PL peak (Figure 3, left panel). More efforts on improving the size distribution of such small core dots are in place to solve this problem.

A purification scheme for the zinc-blende core nanocrystals was identified as a key issue in optimization of PL QY of the zinc-blende core/shell nanocrystals (Figure 3, right panel). Synthesis with the optimized core purification procedure described above was quite reproducible and yielded nanocrystals with high optical quality. Figure 3 (right panel, solid symbols linked with solid lines) illustrates the results associated with four parallel syntheses, which reveals good reproducibility for the typical synthetic scheme described in this work. It should be pointed out that the reproducibility was further confirmed by different operators and/or using different batches of zinc-blende core nanocrystals.

Conversely, the traditional purification scheme developed for wurtzite CdSe nanocrystals,[13] hexane–methanol extraction either with or without following acetone precipitation, did not yield nanocrystals with high optical quality (Figure 3, right panel). This difference should be a result of the solution composition difference between two cases. Different from zinc-blende CdSe nanocrystals synthesis, typical synthesis of wurtzite core nanocrystals usually required a large amount of fatty amine in the solution, and the selenium precursor was a soluble compound, i.e., the Se–tributylphosphine complex. The results shown in Figure 3 (right panel) imply that removal of both types of precursor residuals for CdSe core nanocrystals, i.e., cadmium fatty acid salts and elemental selenium, by converting them to soluble species in methanol during the core purification step was essential for the reproducible synthesis of zinc-blende CdSe/CdS core/shell nanocrystals with high optical quality.

Morphology, Size, and Crystal Structure of the Core/Shell Nanocrystals with Zinc-Blende CdSe Cores. As shown in Figure 4, the morphology of the CdSe/CdS core/shell nanocrystals using zinc-blende CdSe cores was maintained to be dot-shaped. Upon the growth of the CdS shell, the increase of the particle size was evidenced by TEM measurements. The increase of average thickness observed in TEM pictures approximately matched the targeted number of CdS monolayers by each growth cycle. All core/shell nanocrystals retained the nearly monodisperse size distribution of the core nanocrystals (Figure 4, bottom), which is consistent with the narrow fwhm of PL peaks discussed above (Figure 2).

The XRD patterns in Figure 5 revealed that when zinc-blende CdSe cores were employed and growth was performed under the typical reaction temperatures (Figure 1), both CdSe and CdSe/CdS core/shell nanocrystals possessed zinc-blende crystal structure. Although there are some overlapping peaks between zinc-blende and wurtzite structures for a given material, each crystal structure possesses its own unique signatures.[31] For the zinc-blende crystal structure, its (400) and (331) peaks are clearly distinguishable features. For the wurtzite crystal structure, the (102), (103), and (203) peaks can be regarded as the comparative unique peaks for the structure (see more discussions on wurtzite structure below).

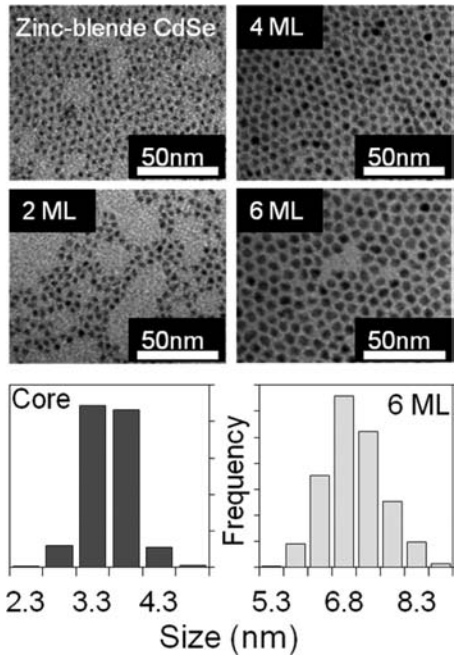

Figure 4. TEM images and size distribution histograms of the zinc-blende CdSe core and the corresponding CdSe/CdS core/shell nanocrystals with a given number of monolayers (ML) of the CdS shell.

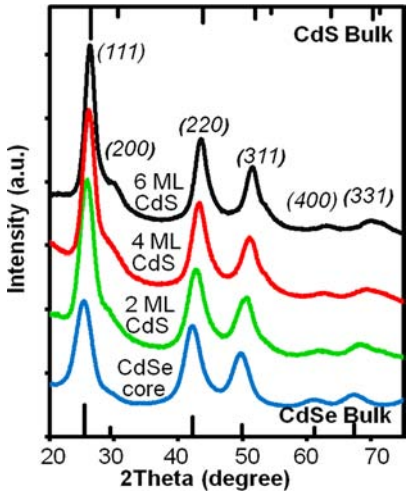

Figure 5. XRD patterns of the zinc-blende CdSe core (diameter = 3.5 nm) and the corresponding core/shell nanocrystals with different numbers of CdS monolayers. The standard diffraction patterns of zinc-blende bulk CdSe (red vertical lines at the bottom) and CdS (black vertical lines at the top) are included as references (PDF of CdSe: 65-2891, CdS: 65-2887).

As the shell thickness increased, the diffraction peak positions gradually shifted from those of zinc-blende CdSe to those of zinc-blende CdS. With 4–6 monolayers of CdS grown onto the surface of CdSe core nanocrystals, the final XRD pattern shifted to the expected one for zinc-blende CdS. This implies the outer CdS shell was sufficiently thick to dominate the lattice structure of the core/shell nanocrystals.

The results in Figure 5 indicate that, under proper conditions, CdSe/CdS core/shell nanocrystals could inherit the zinc-blende crystal structure of the core nanocrystals. It was reported that, during the growth of CdS shell, zinc-blende CdSe

dx.doi.org/10.1021/ja306651x | J. Am. Chem. Soc. 2012, 134, 19685–19693

core nanocrystals were found to be readily converted to wurtzite structure, and primary amine was often suspected to cause the conversion.[17,19,20] With the current synthetic scheme, a substantial amount of primary amine in the reaction solution (with a concentration of up to 50% in volume) did not cause a problem for retaining the zinc-blende crystal structure. In comparison to the systems used in the literature, single precursor and low reaction temperatures in our system were two apparent differences. To distinguish these two factors, reactions with the same single precursor but relatively high reaction temperatures were performed. Experimental results clearly revealed the evidence for the appearance of wurtzite features for the resulting core/shell nanocrystals at a temperature above 200 °C (see Figure S2, Supporting Information).

High-resolution transmission electron microscopy (HR-TEM) studies revealed that the zinc-blende core/shell nanocrystals were single crystalline. Though the core/shell nanocrystals grown at typical reaction temperatures inherited the zinc-blende structure of the core CdSe nanocrystals, the core/shell nanocrystals did possess some stacking faults (Figure 6, right panel). Approximately, there were 1−2 stacking faults

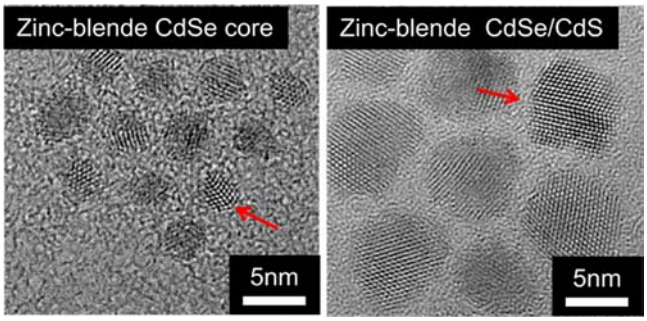

Figure 6. HR-TEM images of the zinc-blende CdSe core and CdSe/CdS core/shell nanocrystals. The red arrow indicates a twin stacking fault for each case.

on average per core/shell nanocrystal. Examination of the core nanocrystals under HR-TEM (Figure 5, left) revealed that such stacking faults existed for the core nanocrystals as well, which is consistent with a detailed analysis reported in the literature.[32] These results suggest that the stacking faults in the core/shell nanocrystals were likely inherited from the core nanocrystals. To synthesize defect-free zinc-blende CdSe/CdS core/shell nanocrystals, it would be necessary to further improve the quality of the zinc-blende core nanocrystals.

Growth of CdSe/CdS Core/Shell Nanocrystals Using Wurtzite CdSe Cores. This subject has been studied quite intensively in the field.[11,13,14,33] To the best of our knowledge, however, epitaxial growth of the CdS shell onto wurtzite CdSe core nanocrystals has not been carried out in the temperature range below 150 °C using a single precursor. For this reason, it is necessary to carry out a comparative study of CdS shell growth using wurtzite CdSe core nanocrystals with the same growth conditions outlined above.

The wurtzite CdSe cores used for the comparative study were synthesized using the literature method.[13] The TEM images (Figure 7, left panel), XRD patterns (Figure 7, right panel), and evolution of the UV−vis and PL spectra (Figure S3, Supporting Information) all confirmed that the typical synthetic conditions outlined above also worked well for the growth of the wurtzite CdSe/CdS core/shell nanocrystals. The properties

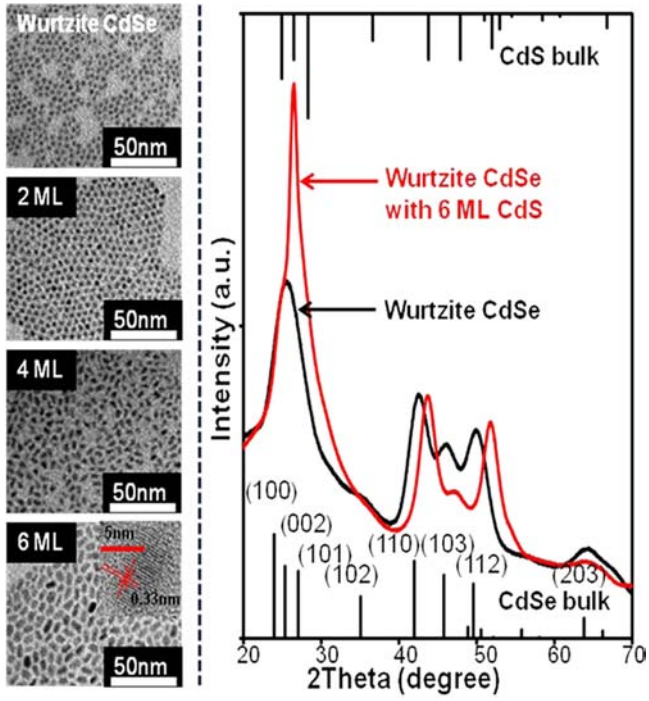

Figure 7. Left panel: TEM images of wurtzite CdSe core nanocrystals and the corresponding CdSe/CdS core/shell nanocrystals with 2, 4, and 6 monolayers of CdS shell. Right panel: XRD patterns of wurtzite CdSe core nanocrystals and CdSe/CdS core/shell nanocrystals with 6 monolayers of CdS shell. The standard diffraction patterns of wurtzite bulk CdSe (black vertical lines at the bottom) and CdS (black vertical lines at the top) are included as references (PDF of CdSe: 65-3415, CdS: 65-3414).

of the resulting CdSe/CdS core/shell nanocrystals were similar to those grown at around 240 °C using cadmium fatty acid salts and elemental S as the precursors.[13]

During the growth of the CdS shell, the morphology of the nanocrystals changed gradually from dot-shaped to elongated-shaped (Figure 7, left). Furthermore, HR-TEM studies revealed that the elongation direction of the rod-shaped CdSe/CdS core/shell nanocrystals was along the *c*-axis of the wurtzite crystal structure (see Figure 7 left, inset in the bottom TEM picture).

Overall, in comparison to the literature,[13] the lower growth temperatures used in this work (≤140 °C versus ≥200 °C) did not affect the structure feature and the general optical properties of the resulting wurtzite CdSe/CdS core/shell nanocrystals. These results seemed to be reasonable. It is well-known that, for bulk CdSe and CdS crystals, wurtzite structure is the high-temperature stable phase, which should thus be less sensitive to the elevated growth temperatures used previously.

The influence of crystal structure on PL QY and PL peak fwhm evolution (see Figure S1 in Supporting Information and Figure 2 for comparison, and also see discussions related to Figure S1 and Figure 2) between zinc-blende core/shell dots and their wurtzite counterparts synthesized under similar conditions was evident. Experimental results to be discussed below shall further reveal other interesting differences in optical properties between zinc-blende CdSe/CdS core/shell nanocrystals and their wurtzite counterparts.

Unique PL Decay Kinetics of Zinc-Blende CdSe/CdS Core/Shell Nanocrystals. Figure 8 (left panel) illustrates PL

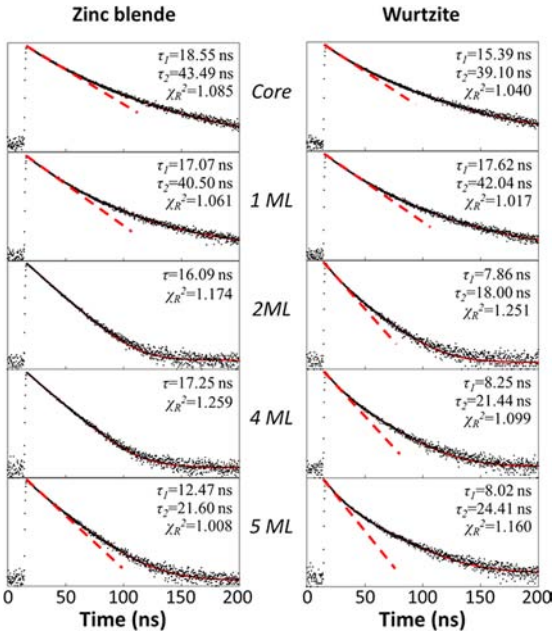

Figure 8. Left panel: PL decay kinetics of zinc-blende CdSe core and CdSe/CdS core/shell nanocrystals. Right panel: PL decay kinetics of wurtzite CdSe core and CdSe/CdS core/shell nanocrystals. For all curves, the *y*-axis was in logarithm, and the peak counts were fixed as 5000. The red solid line is single-exponential or double-exponential fitting results (with lifetime values and the goodness-of-fit at the top right corner for each plot). If all the data could not be well fitted as single-exponential kinetics, a red dashed line was added as the linear fitting curve for the first few data points. Note: the flat tail in some of the data traces was background signals and was well fitted with the instrument software.

decay results of zinc-blende CdSe/CdS core/shell nanocrystals. For comparison, wurtzite CdSe/CdS core/shell nanocrystals were also measured under the same conditions (Figure 8, right panel), which can be well fitted into a double-exponential decay function similar to what is reported in the literature.[34−36]

Conversely, zinc-blende CdSe/CdS core/shell nanocrystals behaved differently. For the series of samples shown in Figure 8 (left panel), when the shell thickness was 2 to 4 monolayers of CdS, the PL decay could be well fitted into a single-exponential decay function. Generally, single-exponential PL decay was quite reproducibly observed for zinc-blende CdSe/CdS core/shell nanocrystals with 2, 3, and 4 monolayers of the CdS shell, with 3 and 4 monolayers giving the best reproducibility and not as good for the samples with 2 monolayers of the CdS shell.

To verify the unusual single-exponential PL decay, the peak photon counts were set at a reasonably high value, i.e., 5000 photons, for each measurement. The excitation pulse peak power was varied between 1 and 0.1 W/cm^2. The optical density for the solution samples was set to be significantly below 0.1 to avoid possible energy transfer. The goodness-of-fit (χ^2_R) was set not greater than 1.300, and all fitting parameters are summarized in Table S1 (Supporting Information). Multiple measurements per sample and multiple samples for the same shell thickness from different syntheses were employed for the measurements. All measurements were carried out at room temperature.

To our knowledge, the ensemble PL decay of wurtzite CdSe/CdS core/shell nanocrystals reported in the literature was multiple-exponential (mostly double-exponential) decay.[35−37] Measurements performed with single-dot spectroscopy revealed that, in a given sample, some of the wurtzite dots were single-exponential, and some of them were multiple-exponential.[38] For wurtzite CdSe/CdS core/shell nanocrystals, those single dots with single-exponential PL decay typically had a lifetime of ∼8 ns,[39] which is similar to the fast component for the wurtzite CdSe/CdS core/shell dots with 2−5 monolayers of CdS (see the τ_1 values in Figure 8, right panel). Conversely, the single-exponential lifetime observed for ensemble PL of zinc-blende CdSe/CdS core/shell nanocrystals (∼16 ns) was about twice as long (see fitting results in Figure 8, left panel).

Experiments are actively in place to identify the nature of the single-exponential PL decay kinetics for the zinc-blende CdSe/CdS core/shell nanocrystals. Preliminary results revealed that, while a typical zinc-blende CdSe/CdS core/shell nanocrystal sample with 4-monolayer CdS shell possessed an ensemble single-exponential lifetime being about 16 ns, the PL decay usually became double-exponential with an additional fast component (Figure 9, right panel) if the nanocrystals were

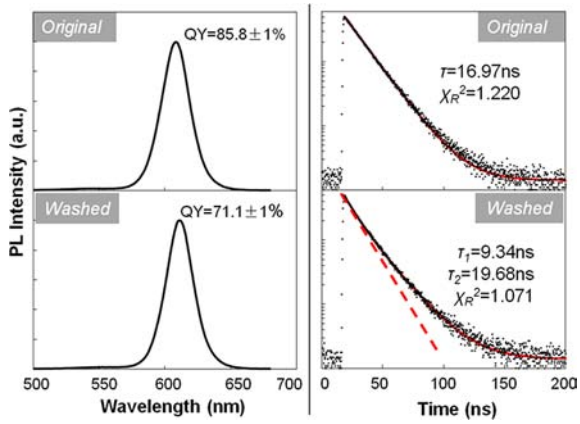

Figure 9. PL spectra (left panel) and PL decay kinetics (right panel) of zinc-blende core/shell nanocrystals with 4 monolayers of CdS shell before (top) and after (bottom) washing to remove some of the surface ligands. The red solid line (red dashed line) is the fitting results for the entire data series (for the first few data points). The PL QY was based on at least 10 different measurements for each sample.

washed multiple times to remove some of the surface ligands. At the same time, the PL QY would decrease a bit (Figure 9, left panel) from its typical value by the partial removal of the surface ligands. Furthermore, decrease of PL QY and departure from single-exponential PL decay kinetics both became more and more pronounced as more surface ligands were removed.

The preliminary results described above suggest that the PL decay channel with ∼16 ns lifetime should be the intrinsic PL decay for the zinc-blende CdSe/CdS core/shell nanocrystals. This hypothesis is supported by the other results presented above. First, when the CdS shell was grown onto the zinc-blende CdSe core nanocrystals, the surface decay channel—the other component observed for the zinc-blende core nanocrystals in Figure 8 (top left)—was gradually removed. Second, the PL peak fwhm decreased about 30% upon the growth of the CdS shell onto the zinc-blende CdSe nanocrystals (Figure 2, bottom right), which is consistent with the elimination of a PL decay channel. Third, the PL QY increase upon the growth of the CdS shell as shown in Figure 2 (right top) is also consistent with the elimination of the surface PL decay channel as the surface channel should possess a low PL QY. Fourth, as described above, addition of cadmium oleate into the reaction

solution was most effective for the zinc-blende core and core/shell nanocrystals with 1−2 monolayers of CdS on the surface in terms of improving their PL QY, which implies that the radiative recombination center of excitons in zinc-blende nanocrystals gradually shifted away from the surface upon the CdS shell growth.

CONCLUSION

CdSe/CdS core/shell nanocrystals were found to faithfully inherit the original crystal structures of the core nanocrystals, i.e., both zinc-blende and wurtzite CdSe/CdS core/shell nanocrystals being successfully synthesized using the corresponding core nanocrystals. A relatively low shell growth temperature, i.e., between 100 and 140 °C, was identified as the key parameter for successful epitaxial growth of the zinc-blende core/shell nanocrystals. Instead of converting the crystal structure, the primary amine under the chosen reaction conditions was found to lower the shell growth temperature to the desirable range by activating the single precursor (cadmium diethyldithiocarbamate) and acted as a dynamic surface ligand to balance growth and colloidal stability. The optical properties of zinc-blende CdSe/CdS core/shell nanocrystals were found to be substantially different from their wurtzite counterparts. Generally, the zinc-blende ones could be made with significantly higher PL QY than that of their wurtzite counterparts, and zinc-blende core/shell nanocrystals with proper shell thickness showed single-exponential PL decay dynamics. Preliminary results further indicate that, by some modifications, this scheme could also be used for synthesis of zinc-blende CdSe/CdS core/shell nanocrystals with a thicker shell to offer stable and nonblinking yet bright quantum dot emitters. Although much more work is needed to study these interesting quantum dots, zinc-blende CdSe/CdS core/shell nanocrystals reported here could be considered as one step further toward synthesis of "optical monodisperse" quantum dots. As synthetic chemistry of colloidal nanocrystals moves into building "artificial nanocrystals" through "bandgap and composition engineering on a single nanocrystal",[40] chemical insights on crystal structure control revealed by this work should be of importance for the field of materials chemistry.

EXPERIMENTAL SECTION

Chemicals. Stearic Acid (HSt, 90+%), tetramethylammonium hydroxide (98%), octylamine (98%), cadmium oxide (CdO, 99.998%), selenium powder (Se, 200mesh, 99.999%), octadecyamine (98%), octane (99%), 1-octadecene (ODE, 90%), and oleic acid (HOl, 90%) were purchased from Alfa-Aesar. Tributylphosphine (TBP) was purchased from Shanghai Titan Chem. Cadmium acetate dihydrate ($Cd(Ac)_2{\cdot}2H_2O$, 98.5%) was purchased from Shanghai Tingxin Reagents. Trioctylphosphine oxide (TOPO, tech, 90%) was purchased from Aldrich. Sodium diethyldithiocarbamate trihydrate ($NaDDTC{\cdot}3H_2O$, 99%) was purchased from Aladdin Reagents. Oleylamine (C_{18} content 80−90%) was purchased from Acros. All organic solvents were purchased from Sinopharm Reagents. All chemicals were used directly without any further purification unless otherwise stated.

Synthesis of Cadmium Stearate ($Cd(St)_2$). The synthetic procedure was based on the synthesis of $Mn(St)_2$ reported in the literature.[41] Typically, HSt (20 mmol) was neutralized with equal-mole of tetramethylammonium hydroxide in 200 mL of methanol. Into this solution, $Cd(Ac)_2{\cdot}2H_2O$ (10 mmol) dissolved in 50 mL of methanol was added dropwise under vigorous stirring. White $Cd(St)_2$ immediately precipitated, and the mixture was stirred for another 20 min after dropping to ensure the reaction was completed. Subsequently, the white precipitate was collected through filtration and then washed three times with methanol. The final product was obtained by drying under vacuum overnight.

Synthesis of Cadmium Diethyldithiocarbamate ($Cd(DDTC)_2$). With a procedure modified from the synthesis of $Zn(DDTC)_2$,[25] $Cd(Ac)_2{\cdot}2H_2O$ (10 mmol) was dissolved with 100 mL of distilled water in a 400 mL beaker. Into this solution, $NaDDTC{\cdot}3H_2O$ (20 mmol) dissolved in 60 mL of distilled water was added dropwise under vigorous stirring. White precipitates of $Cd(DDTC)_2$ quickly formed. The mixture was stirred for another 20 min after mixing to ensure the reaction was completed. The white precipitate was separated from the solution phase by filtration and washed three times with distilled water. The final product in white powder form was obtained by drying under vacuum overnight. For each shell growth reaction, a 3 mL $Cd(DDTC)_2$-amine-octane solution (0.1 mmol/mL) was prepared by dissolving 0.1227 g of $Cd(DDTC)_2$ in a mixture of octane (1.5 mL), oleylamine (0.45 mL), and octylamine (1.05 mL).

Preparation of Cadmium Oleate ($Cd(Ol)_2$) Solution. CdO (0.1284 g), HOl (1.1299 g), and ODE (6.8917 g) were mixed in a 25 mL flask. After stirring and argon bubbling for 10 min, the flask was heated to 240 °C to get a clear solution.

Synthesis of Zinc-Blende CdSe Core and Wurtzite CdSe Core Nanocrystals. Zinc-blende CdSe nanocrystals were synthesized using a modified procedure reported by Cao's group.[15] In a typical synthesis, $Cd(St)_2$ (0.1356 g, 0.2 mmol) and Se powder (0.0079 g, 0.1 mmol) were loaded into a 25 mL three-neck flask with 4 mL of ODE. After stirring and argon bubbling for 10 min, the flask was heated to 240 °C at a heating rate of 40 °C/min. Needle tip aliquots were taken for UV−vis and PL measurements to monitor the reaction. When the targeted size of nanocrystals was achieved, the reaction mixture was allowed to cool to 50 °C, and an in situ purification procedure described below was employed to purify the nanocrystals.

Wurtzite CdSe nanocrystals were made by a procedure modified from the previous literature.[13] For a typical reaction, the mixture of $CdSt_2$ (0.0678 g, 0.1 mmol), octadecyamine (0.75 g), TOPO (0.25 g), and 4 mL of ODE in a 25 mL three-neck flask was bubbled with argon for 10 min at both room temperature and 100 °C and then heated to 260 °C to obtain a colorless clear solution. Into this hot solution was quickly injected a selenium solution (1 mL) made by dissolving 1 mmol of Se in 0.236 g of TBP in a glovebox and further diluted with 0.69 g of ODE. The growth temperature was then dropped to about 240 °C. Aliquots were taken from the solution to monitor the reaction. When the targeted size of nanocrystals was obtained, the reaction mixture was allowed to cool down to 50 °C, and an in situ purification procedure described below was employed to purify the nanocrystals.

In Situ Purification Schedule for Core Nanocrystals. To ensure the reproducibility of epitaxial growth, an in situ purification procedure was developed for preparation of core nanocrystals in the reaction flask. For zinc-blende core nanocrystals, tributylphosphine (0.2 mL), octylamine (0.2 mL), hexane (3 mL), and methanol (6 mL) were added to the reaction solution at 50 °C and stirred for 2 min. Tributylphosphine was used to get rid of the unreacted elemental Se,[27] which was found to be essential for achieving reproducible core/shell growth for zinc-blende dots. After stirring was turned off, the colorless methanol layer was separated from the top ODE/hexane layer by syringe. This extraction procedure was repeated four times, but tributylphosphine was only added for the first and third runs. The hexane left in the ODE layer was removed by argon bubbling at about 60 °C. For wurtzite core nanocrystals, a similar extraction procedure was performed, but neither tributylphosphine nor octylamine was added.

Synthesis of CdSe/CdS Core/Shell Nanocrystals. In a typical synthesis, a mixture of octane (2 mL), octylamine (2.1 mL), and oleylamine (0.9 mL) was heated to 60 °C in a three-neck flask under argon flow, and then about 1 mL of purified CdSe (with zinc-blende or wurtzite crystal structure) core solution (containing about 1×10^{-7} mol of nanocrystals estimated by their extinction coefficients[28]) was added to this flask. The amount of precursor solution for each injection was estimated using a procedure suggested in the literature[25] and calibrated by the TEM measurements. For example, for a reaction with 1×10^{-7} mol of CdSe (diameter: 3.5 nm) nanocrystals, the

amount for six consecutive injections of the $Cd(DDTC)_2$-amine-octane solution was calibrated as 0.09, 0.12, 0.16, 0.20, 0.25, and 0.31 mL, respectively. To allow the growth of the first monolayer of CdS, after the $Cd(DDTC)_2$ precursor solution was injected via syringe to this reaction flask, the reaction mixture was immediately heated to 140 °C in 5 min and kept for another 20 min. After growth of the first monolayer of the shell, the reaction mixture was allowed to cool down to 80 °C, and the second injection of the $Cd(DDTC)_2$ precursor solution was applied. This reaction cycle, addition of the precursor solution at 80 °C and growth by heating the solution at a targeted temperature (140 °C for typical synthesis) for about 20 min, was continued until a targeted number of CdS monolayers were obtained. The growth temperature could be further decreased by increasing the concentration of amine in the reaction mixture.

Washing Procedure for Reducing Surface Ligand Coverage of the Final CdSe/CdS Nanocrystals for PL QY and PL Decay Measurements (Figure 9). Typically, the final raw solution (0.5 mL) was taken from a three-neck bottom flask to a 4 mL glass vial, and hexane (0.5 mL), methanol (1.25 mL), and 0.3 mL of ODE were added for the first washing. Then the solution was heated to 50 °C. After vortex and centrifugation, the bottom methanol layer was removed with a syringe at 50 °C. This washing, extraction, and separation procedure was repeated six times for the sample used for the measurements related to Figure 9, and no ODE was added for the consecutive washing operation.

Optical Measurements. UV−vis spectra were taken on an Analytik Jena S600 UV−visible spectrophotometer. Photoluminescence spectra were measured using a Tianjing GangDong F380 Fluorometer. The absolute PL QY was measured using an integrating sphere coupled with a QE65000 spectrometer from Ocean Optical Co. Ltd. The nanocrystal sample was diluted to gradient values of optical density being below 0.1, and multiple measurements were performed for each sample after the diluted solutions were equilibrated at room temperature. The accuracy and stability of the system was verified by laser dyes with known PL QY.

Transmission Electron Microscopy (TEM) and High-Resolution TEM (HR-TEM). TEM images were taken on a JEOL JEM-1200EX transmission electron microscope with an acceleration voltage of 80 kV using copper grids coated with pure carbon support film (400-mesh). HR-TEM pictures were taken on a JEOL JEM-2100 microscope with an acceleration voltage of 200 kV using a copper grid coated with ultrathin carbon film as the substrates.

X-ray Powder Diffraction (XRD). XRD patterns were acquired using a Rigaku Ultimate-IV X-ray diffractometer operating at 40 kV/40 mA using Cu Kα line (λ = 1.5418 Å). Since the reaction mixture contained a large percentage of solid reactants and side products at room temperature, purification was needed to ensure the diffraction patterns with good quality. After the reaction solution was transferred into a separating funnel, extra ODE was added. Into this mixture, hexane and methanol (volume ratio = 1:2) were added to form a biphase system, and the bottom colorless methanol solution was discarded. This extraction procedure was repeated three times (ODE was necessary only for the first time). The nanocrystals were precipitated with addition of acetone after extraction, and the precipitate was separated by decantation of the solution waste and applied directly onto a glass slide for XRD measurements.

PL Decay Dynamics. PL decay curves were measured at room temperature on a time-correlated single-photon counting (TCSPC) spectrofluorometer (FL900, Edinburgh Instrument, UK). The samples were excited by a 405 nm picosecond laser diode with a repetition rate of 2 MHz. For all measurements, the *y*-axis was in logarithm; the peak photon counts were fixed as 5000; and either single-exponential or double-exponential fitting results were obtained with a goodness-of-fit being smaller than 1.300.

■ ASSOCIATED CONTENT

Supporting Information

Additional figures and table. This material is available free of charge via the Internet at http://pubs.acs.org.

■ AUTHOR INFORMATION

Corresponding Author

hattieqin@zju.edu.cn; xpeng@zju.edu.cn

Notes

The authors declare no competing financial interest.

■ ACKNOWLEDGMENTS

We are grateful for the help from Prof. Wenjun Dong and Mr. Qingtang Sun on HR-TEM measurements and Dr. Wei Fang, Mr. Liang Hu, and Mr. Kewei Wu on PL lifetime measurements. We are grateful for the financial support from the National Natural Science Foundation of China (NSFC, No. 21233005).

■ REFERENCES

(1) Murray, C. B.; Kagan, C. R.; Bawendi, M. G. *Annu. Rev. Mater. Sci.* **2000**, *30*, 545.
(2) Peng, X. G. *Nano Res.* **2009**, *2*, 425.
(3) Talapin, D. V.; Rogach, A. L.; Kornowski, A.; Haase, M.; Weller, H. *Nano Lett.* **2001**, *1*, 207.
(4) Qu, L. H.; Peng, X. G. *J. Am. Chem. Soc.* **2002**, *124*, 2049.
(5) Schlamp, M. C.; Peng, X. G.; Alivisatos, A. P. *J. Appl. Phys.* **1997**, *82*, 5837.
(6) Bruchez, M.; Moronne, M.; Gin, P.; Weiss, S.; Alivisatos, A. P. *Science* **1998**, *281*, 2013.
(7) Chan, W. C. W.; Nie, S. M. *Science* **1998**, *281*, 2016.
(8) Klimov, V. I.; Mikhailovsky, A. A.; Xu, S.; Malko, A.; Hollingsworth, J. A.; Leatherdale, C. A.; Eisler, H. J.; Bawendi, M. G. *Science* **2000**, *290*, 314.
(9) Coe, S.; Woo, W. K.; Bawendi, M.; Bulovic, V. *Nature* **2002**, *420*, 800.
(10) Hines, M. A.; Guyot-Sionnest, P. *J. Phys. Chem.* **1996**, *100*, 468.
(11) Peng, X. G.; Schlamp, M. C.; Kadavanich, A. V.; Alivisatos, A. P. *J. Am. Chem. Soc.* **1997**, *119*, 7019.
(12) Dabbousi, B. O.; RodriguezViejo, J.; Mikulec, F. V.; Heine, J. R.; Mattoussi, H.; Ober, R.; Jensen, K. F.; Bawendi, M. G. *J. Phys. Chem. B* **1997**, *101*, 9463.
(13) Li, J. J.; Wang, Y. A.; Guo, W. Z.; Keay, J. C.; Mishima, T. D.; Johnson, M. B.; Peng, X. G. *J. Am. Chem. Soc.* **2003**, *125*, 12567.
(14) Chen, Y.; Vela, J.; Htoon, H.; Casson, J. L.; Werder, D. J.; Bussian, D. A.; Klimov, V. I.; Hollingsworth, J. A. *J. Am. Chem. Soc.* **2008**, *130*, 5026.
(15) Yang, Y. A.; Wu, H.; Williams, K. R.; Cao, Y. C. *Angew. Chem.* **2005**, *117*, 6870.
(16) Lim, S. J.; Chon, B.; Joo, T.; Shin, S. K. *J. Phys. Chem. C* **2008**, *112*, 1744.
(17) Mahler, B.; Lequeux, N.; Dubertret, B. *J. Am. Chem. Soc.* **2010**, *132*, 953.
(18) Chen, G. J.; Zhang, W. J.; Zhong, X. H. *Front. Chem. China* **2010**, *5*, 214.
(19) Xia, X.; Liu, Z. L.; Du, G. H.; Li, Y. B.; Ma, M. *J. Lumin.* **2010**, *130*, 1285.
(20) Xia, X.; Liu, Z. L.; Du, G. H.; Li, Y. B.; Ma, M. *J. Phys. Chem. C* **2010**, *114*, 13414.
(21) Wang, X. Y.; Ren, X. F.; Kahen, K.; Hahn, M. A.; Rajeswaran, M.; Maccagnano-Zacher, S.; Silcox, J.; Cragg, G. E.; Efros, A. L.; Krauss, T. D. *Nature* **2009**, *459*, 686.
(22) Mahler, B.; Spinicelli, P.; Buil, S.; Quelin, X.; Hermier, J. P.; Dubertret, B. *Nat. Mater.* **2008**, *7*, 659.
(23) Pradhan, N.; Reifsnyder, D.; Xie, R. G.; Aldana, J.; Peng, X. G. *J. Am. Chem. Soc.* **2007**, *129*, 9500.
(24) Protiere, M.; Reiss, P. *Nanoscale Res. Lett.* **2006**, *1*, 62.
(25) Chen, D. A.; Zhao, F.; Qi, H.; Rutherford, M.; Peng, X. G. *Chem. Mater.* **2010**, *22*, 1437.
(26) Jung, Y. K.; Kim, J. I.; Lee, J. K. *J. Am. Chem. Soc.* **2010**, *132*, 178.
(27) Li, Z.; Peng, X. G. *J. Am. Chem. Soc.* **2011**, *133*, 6578.

(28) Yu, W. W.; Qu, L. H.; Guo, W. Z.; Peng, X. G. *Chem. Mater.* **2003**, *15*, 2854.
(29) Capek, R. K.; Moreels, I.; Lambert, K.; De Muynck, D.; Zhao, Q.; Vantomme, A.; Vanhaecke, F.; Hens, Z. *J. Phys. Chem. C* **2010**, *114*, 6371.
(30) Nag, A.; Kovalenko, M. V.; Lee, J. S.; Liu, W. Y.; Spokoyny, B.; Talapin, D. V. *J. Am. Chem. Soc.* **2011**, *133*, 10612.
(31) Murray, C. B.; Norris, D. J.; Bawendi, M. G. *J. Am. Chem. Soc.* **1993**, *115*, 8706.
(32) Chen, O.; Yang, Y. A.; Wang, T.; Wu, H. M.; Niu, C. G.; Yang, J. H.; Cao, Y. C. *J. Am. Chem. Soc.* **2011**, *133*, 17504.
(33) Xie, R. G.; Kolb, U.; Li, J. X.; Basche, T.; Mews, A. *J. Am. Chem. Soc.* **2005**, *127*, 7480.
(34) Bawendi, M. G.; Carroll, P. J.; Wilson, W. L.; Brus, L. E. *J. Chem. Phys.* **1992**, *96*, 946.
(35) Garcia-Santamaria, F.; Brovelli, S.; Viswanatha, R.; Hollingsworth, J. A.; Htoon, H.; Crooker, S. A.; Klimov, V. I. *Nano Lett.* **2011**, *11*, 687.
(36) Brovelli, S.; Schaller, R. D.; Crooker, S. A.; Garcia-Santamaria, F.; Chen, Y.; Viswanatha, R.; Hollingsworth, J. A.; Htoon, H.; Klimov, V. I. *Nat. Commun.* **2011**, *2*, 280.
(37) Pal, B. N.; Ghosh, Y.; Brovelli, S.; Laocharoensuk, R.; Klimov, V. I.; Hollingsworth, J. A.; Htoon, H. *Nano Lett.* **2012**, *12*, 331.
(38) Schlegel, G.; Bohnenberger, J.; Potapova, I.; Mews, A. *Phys. Rev. Lett.* **2002**, *88*, 137401.
(39) Spinicelli, P.; Buil, S.; Quelin, X.; Mahler, B.; Dubertret, B.; Hermier, J. P. *Phys. Rev. Lett.* **2009**, *102*, 136801.
(40) Peng, X. G. *Acc. Chem. Res.* **2010**, *43*, 1387.
(41) Chen, Y. F.; Johnson, E.; Peng, X. G. *J. Am. Chem. Soc.* **2007**, *129*, 10937.